PHARMA SCIENCE MONITOR

AN INTERNATIONAL JOURNAL OF PHARMACEUTICAL SCIENCES

THREE-DIMENSIONAL QUANTITATIVE STRUCTURE-ACTIVITY RELATIONSHIP AND COMPARATIVE MOLECULAR FIELD ANALYSIS OF CYP450 ENZYME SYSTEM INHIBITORS

Ravi Shekar Ananthula*, Swetha Gade, S.K. Mahmood

Bioinformatics Division, Environmental Microbial Laboratory Department of Botany, Osmania University, Hyderabad, Andhra Pradesh 500007, India

ABSTRACT

"cytochrome P450" family of enzymes are present in every cell and are responsible for biotransformation of drugs from active to inactive metabolites that are readily excreted by the body., the rapid metabolism of certain drugs by the CYP450 enzyme system can markedly alter their pharmacokinetic (PK) profile and can result in sub-therapeutic plasma levels of those drugs over time. To understand the ligand structural requirements and to enhance inhibitory potency for new ligands against CYP-450 enzyme system, 3D–QSAR comparative molecular field analysis (CoMFA) study was carried out on a series of 2-[3-(4-fluorobenzyl)-5-pyridin-4-yl-1H-pyrazol-1-yl] derivatives, as selective CYP-450 enzyme system inhibitors. Comparative molecular field analysis (CoMFA) QSAR models were computed with Sybyl 6.7v. The developed model gave leave–one–out (LOO) cross–validated correlation coefficient $q2$ value of 0.844, non–cross–validated correlation coefficient $r2$ value of 0.992, and the predicted correlation coefficient $r2_{pred}$ was found to be 0.781. The QSAR model gave satisfactory statistical results in terms of $q2$ and $r2$ values. The CoMFA model provided the most significant correlation of steric and electrostatic fields with biological activities. The information derived from this study provides a tool for guiding further structural modification to obtain selective inhibitors of CYP450.

Keywords: 3D-QSAR; CoMFA; CoMSIA; cytochrome P450 ; CYP3A4; 2-[3-(4-fluorobenzyl)-5-pyridin-4-yl-1H-pyrazol-1-yl] derivatives; Ligand based drug designing.

INTRODUCTION

The term "cytochrome P450" refers to a family of over 100 enzymes in the human body that modulate various physiologic functions. These CYP enzymes are present in every cell and are responsible for metabolizing or detoxifying consumed foreign (i.e., xeno) biological substances (e.g., toxins, carcinogens, mutagens and drugs) i.e., the

biotransformation of drugs from active to inactive metabolites that are readily excreted by the body. The enzymes primarily involved in drug metabolism are located in the liver. About 30 of these enzymes are primarily located in endoplasmic reticulum of hepatocytes in the liver and in the small intestine, with smaller quantities in the kidneys, lungs and brain. These enzymes play a major role in the metabolism of most drugs commonly used today. Furthermore, the rapid metabolism of certain drugs by the CYP450 enzyme system can markedly alter their pharmacokinetic (PK) profile and can result in sub-therapeutic plasma levels of those drugs over time. In the area of anti-infective therapy, such as treating viral infections such as human immunodeficiency virus (HIV) infections, such sub-therapeutic drug plasma levels can lead to an increase in resistance of the virus. [1]

Cytochrome P450s (CYPs) play a crucial role in metabolism [2]. P450-mediated metabolism is an oxidation reaction that is a part of Phase I metabolic cycle. P450s are the strongest oxidizing agents known in living systems, consequently many drugs can be oxidized by more than one P450 enzyme [3]. These enzymes metabolize a vast array of structurally diverse drugs in market – approximately 90% of all marketed drugs – and are responsible for major routes of drug clearance [3,4]. Members of the CYP family are particularly prone to inhibition because of their broad substrate specificity, which is amenable to competitive inhibition arising from different types of structurally diverse drugs that can be metabolized by the same enzymes[5]. Thus, it has become a widely accepted practice that potent inhibition of these enzymes should be avoided where possible [3].

In drug therapy, CYP inhibition may result in undesirable consequences: 1. an increase of toxicity caused by decreased drug metabolism rate, 2. a decrease in pharmacological effects due to the decreased formation of reactive metabolites of pro-drugs, and 3. drug–drug interactions (DDI) by double medication [5] which lead to a decreased clearance of one of the drugs when two or more drugs are administered simultaneously. It is particularly important to consider the biotransformation and elimination of drugs during

their development to determine their potential interactions with CYPs as early as possible [2].

CYP3A4, one of the key P450s, has been identified and modeled extensively. CYP3A4 accounts for 50–60% of drug metabolisms [3]. Now, it is a common practice in drug discovery to screen out chemicals that possess inhibitory activity against CYP3A4-mediated metabolism in order to predict and manage DDI [6]. In this sense, the high quality in silico models is very useful in ADME/ DDI predictions.

Ritonavir (RTV) is a marketed HIV protease inhibitor (PI) that, due to its ability to inhibit the cytochrome P450 3A4 enzyme, is also used to "boost" the pharmacokinetic exposure of many co-administered anti-retrovirals. However, RTV is associated with clinically significant gastrointestinal and metabolic side effects including nausea, emesis, diarrhea, and dyslipidemia. Administering low doses of a compound with potent antiviral activity may also contribute to the selection of drug-resistant strains of HIV. A novel CYP3A4 inhibitor capable of boosting antivirals as effectively as RTV but devoid of antiviral activity and significant side-effects would offer significant advantages and therapeutic value in the treatment of those suffering from infection with the HIV virus. 2-[3-(4-fluorobenzyl)-5-pyridin-4-yl-1H-pyrazol-1-yl] derivatives are useful in the inhibition of the CYP450 enzyme system and may be used to boost the pharmacokinetic exposure of co-administered drugs, including anti-retrovirals [1]

Quantitative structure–activity relationships (QSARs) are currently acknowledged to be at the heart of the long-term task of systematically evaluation of existing chemicals [7]. Currently, the challenge is to improve the accuracy and predictability of QSAR by taking into account, in a very detailed way, the structural and physicochemical features of the tested compounds.

Since, its introduction in 1988, comparative molecular field analysis (CoMFA) [8] has emerged as one of the most powerful tools in ligand based drug design strategies [9]. The CoMFA methodology assumes that a suitable sampling of steric and electrostatic fields

around a set of aligned molecules provides all the information necessary for understanding their biological properties [10].

The present study aimed at elucidating the structural features of 2-[3-(4-fluorobenzyl)-5-pyridin-4-yl-1H-pyrazol-1-yl] derivatives required for CYP450 enzyme inhibition, and to obtain predictive three-dimensional quantitative structure activity relationship (3D-QSAR) model. The purpose of this study was to present models which predict CYP3A4 inhibitors with molecular descriptors that well represent and easily explain their physicochemical properties with the aim of early identification during the drug development process.

METHODS AND MATERIALS

Molecular modeling:

The three-dimensional structures of 2-[3-(4-fluorobenzyl)-5-pyridin-4-yl-1H-pyrazol-1-yl] derivatives with CYP450 3A4 activity data measured by inhibition of Midazolam metaboloism, were constructed by using SYBYL programming package version 6.7 [11] on a Silicon Graphics Fuel workstation. Energy minimization was performed using tripos force field [12] and the Gasteiger [13] charge with a distance-dependant dielectric and Powell conjugate gradient algorithm with convergence criterion of 0.05 kcal/mol. Further geometric optimization of these compounds was done using the semi-empirical program MOPAC 6.0 and applying the AM1 Hamiltonian [14]. The MOPAC charges were used for entire calculations.
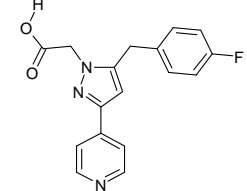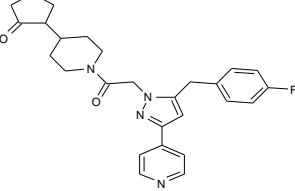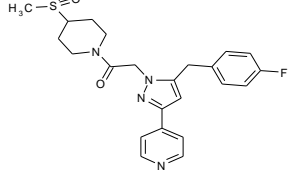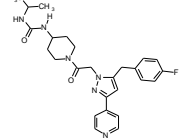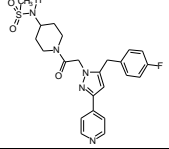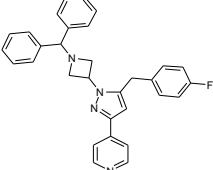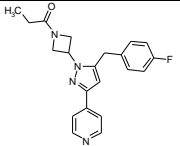
Dataset
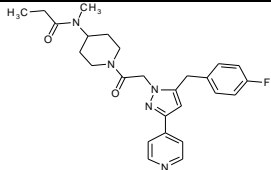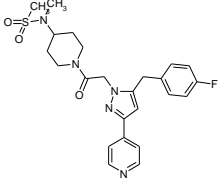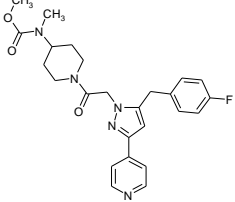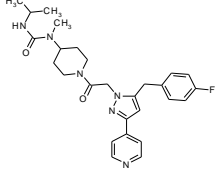
The in vitro biological activity data reported as IC50, for inhibition of CYP450 3A4 by the phenyl ethanolamine compounds were taken from the published work by Planken et al [1]. In vitro inhibitory concentrations (IC50) of the molecules against CYP450 3A4 were converted into corresponding pIC50 [-log(IC50)] and were used as dependent variables in the QSAR calculations.
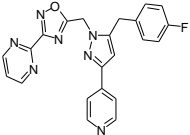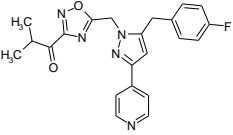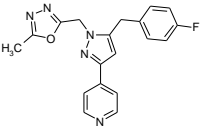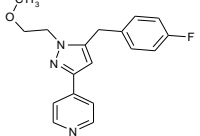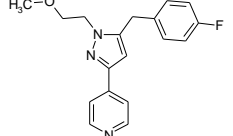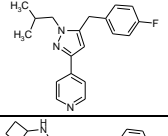
A dataset of 65 2-[3-(4-fluorobenzyl)-5-pyridin-4-yl-1H-pyrazol-1-yl] reported to have CYP450 3A4 inhibitory activities were used for the following QSAR studies (**Table 1**). All the molecules were divided into training set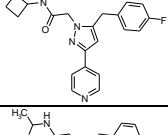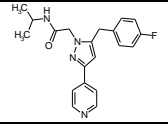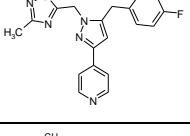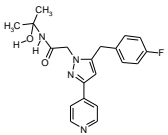 (49 compounds) for generating 3D-QSAR models and a test set (16 compounds) for validating the quality of the models. The test set was selected based on the criteria given by Oprea et al.[15]
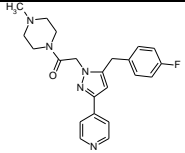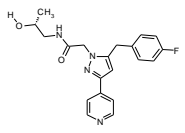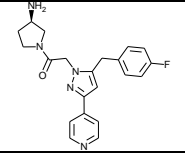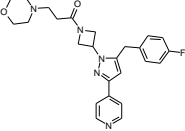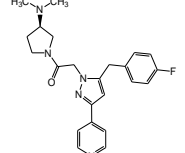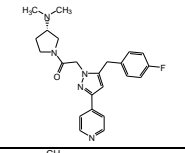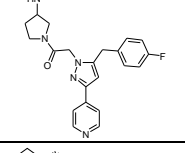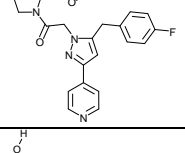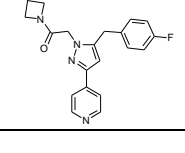
The conformations were generated for the most active compound 25. As the compound is relatively rigid hence we have used systematic search method with a step size of 158 torsion angle to generate the conformational model. The lowest energy conformer was selected and further geometry optimization of each molecule was carried out with MOPAC 6 package using the semi-empirical AM1 Hamiltonian[14]. Optimized structures with MOPAC charges were used for subsequent calculations. This conformer was considered for the building of other molecules.
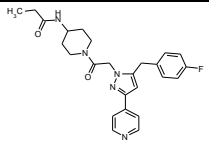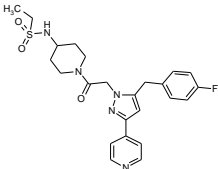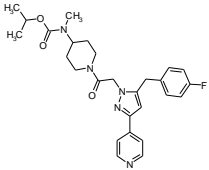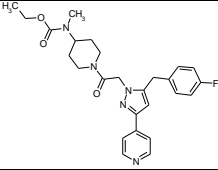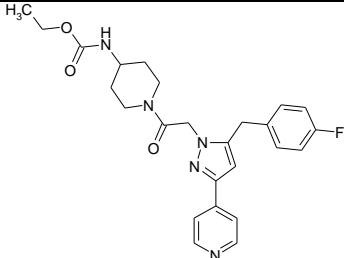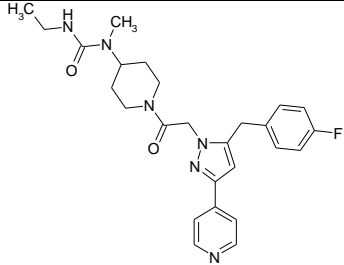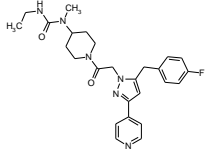
TABLE 1: STRUCTURES AND INHIBITORY ACTIVITIES OF COMPOUNDS USED FOR 3D-QSAR STUDIES
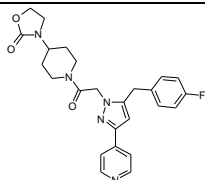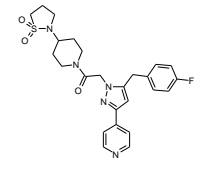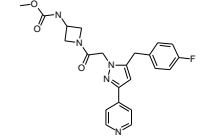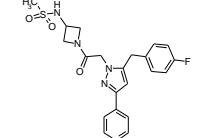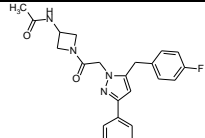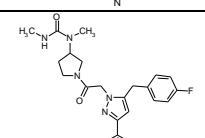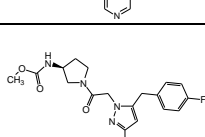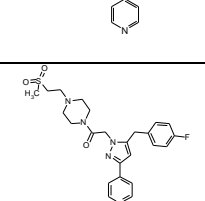
S.No	Name	Structure	CYP3A4 IC50	pIC50
01	[5-(4-fluorobenzyl)-3-pyridin-4-yl-1H-pyrazol-1-yl]acetic c acid		0.094	7.026872
02	1(1-{[5-(4-fluorobenzyl)-3-pyridin-4-yl-1H-pyrazol-1-yl]acetyl}piperidin-4-yl)pyrrolidin-2-one		0.01	8
03	4-(5-(4-fluorobenzyl)-1-{2-[4-(methylsulfonyl)piperidin- 1-yl]-2-oxoethyl}-1H-pyrazol-3-yl)pyridine		0.0218	7.661544
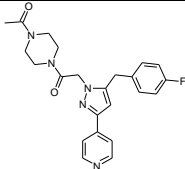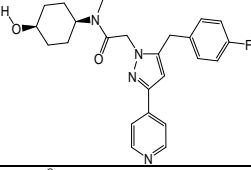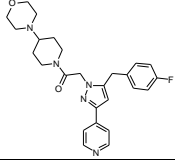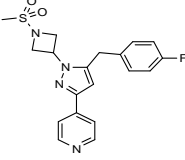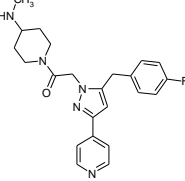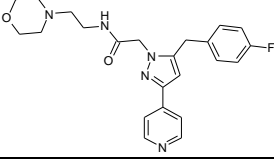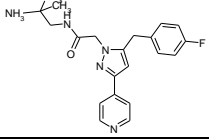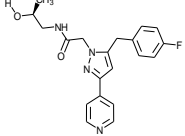
04	N-(1-{[5-(4-fluorobenzyl)-3-pyridin-4-yl-1H-pyrazol-1-yl]acetyl}piperidin-4-yl)-N-methylpropanamide		0.013	7.886057
05	N-(1-{[5-(4-fluorobenzyl)-3-pyridin-4-yl-1H-pyrazol-1-yl]acetylopiperidin-4-yl)-N-methylmethanesulfonamide		0.013	7.886057
06	Methyl (1-{[5-(4-fluorobenzyl)-3-pyridin-4-yl-1H-pyrazol-1-yl]acetyl l}piperidin-4-yl)methylcarbamate		0.009	8.045757
07	N-(1-{[5-(4-fluorobenzyl)-3-pyridin-4-yl-1H-pyrazol-1-yl]acetyl}piperidin-4-yl)-N -isopropyl-N-methyl urea		0.00707	8.150581
08	N-(1-{[5-(4-fluorobenzyl)-3-pyridin-4-yl-1H-pyrazol-1-yl]acetyl}piperidin-4-yl)-N -isopropyl urea		0.0115	7.939302
09	N-(1-{2-[5-(4-fluorobenzyl)-3-pyridin-4-yl-1H-pyrazol-1-yl]acetyl}piperidin-4-yl)methane sulfonamide		0.0138	7.860121
10	4-[1-[1-(diphenylmethyl)azetidin-3-yl]-5-(4-fluorobenzyl)-1H-pyrazol-3-yl]pyridine		0.228	6.642065
11	1-(3-(5-(4-fluorobenzyl)-3-(pyridin-4-yl)-1H-pyrazol-1-yl)azetidin-1-yl)propan-1-one		0.084	7.075721
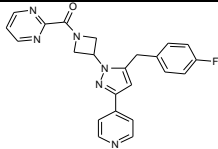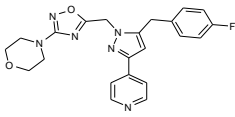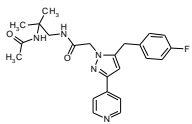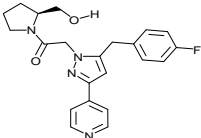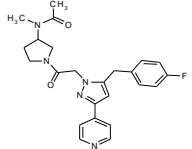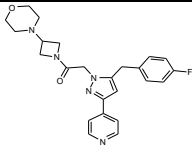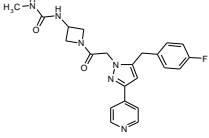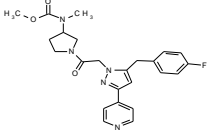
12	2-(5-{[5-(4-fluorobenzyl)-3-pyridin-4-yl-1H-pyrazol-1-yl]methyl}-1,2,4-oxadiazol-3-yl)pyrimidine		0.045	7.346787
13	5-{[5-(4-fluorobenzyl)-3-pyridin-4-yl-1H-pyrazol-1-yl]methyl}-N,N-dimethyl-1,2,4-oxadiazole-3-carboxamide (maleic acid salt)		0.086	7.065502
14	4-{5-(4-fluorobenzyl)-1-[(5-methyl-1,3,4-oxadiazol-2-yl)methyl]-1H-pyrazol-3-yl}pyridine		0.0792	7.101275
15	4-(5-(4-fluorobenzyl)-1-(2-methoxyethyl)-1H-pyrazol-3-yl)pyridine		0.0466	7.331614
16	4-[5-(4-fluorobenzyl)- 1-(2-methoxyethyl)- 1H-pyrazol-3-yl]pyridine		0.0466	7.331614
17	1-[5-(4-fluorobenzyl)- 3-pyridin-4-yl-1H- pyrazol-1-yl]propan-2- ol		0.071	7.148742
18	N-cyclobutyl-2-[5-(4-fluorobenzyl)-3- pyridin-4-yl-1H- pyrazol-1- yl]acetamide		0.028	7.552842
19	2-[5-(4-fluorobenzyl)- 3-pyridin-4-yl-1H- pyrazol-1-yl]- N- isopropylacetamide		0.043	7.366532
20	4-{5-(4-fluorobenzyl)- 1-[(3-methyl-1,2,4- oxadiazol-5-yl)methyl]-1H-pyrazol- 3-yl}pyridine		0.0944	7.025028
21	2-[5-(4-fluorobenzyl)- 3-pyridin-4-yl-1H- pyrazol-1-yl]- N-(2- hydroxy-2-methylpropyl)acetamide		0.02	7.69897

22	1-{[5-(4-fluorobenzyl)- 3-pyridin-4-yl-1H- pyrazol-1-yl]acetyl}-4- methylpiperazine		0.016	7.79588
23	2-[5-(4-fluorobenzyl)- 3-pyridin-4-yl-1H- pyrazol-1-yl]-N-[(2R)- 2-hydroxypropyl]acetamide		0.04	7.39794
24	(3R)-1-{[5-(4- fluorobenzyl)-3-pyridin-4-yl-1H- pyrazol-1-yl]acetyl}pyrrolidin-3- amine		0.059	7.229148
25	4-(3-{3-[5-(4- fluorobenzyl)-3-pyridin-4-yl-1H- pyrazol-1-yl]azetidin- 1-yl}-3-oxopropyl)morpholine		0.042	7.376751
26	(3R)-1-{[5-(4- fluorobenzyl)-3-pyridin-4-yl-1H- pyrazol-1-yl]acetyl}- N,N-dimethylpyrrolidin-3- amine		0.026	7.585027
27	(3S)-1-{[5-(4- fluorobenzyl)-3-pyridin-4-yl-1H- pyrazol-1-yl]acetyl}- N,N-dimethylpyrrolidin-3- amine		0.018	7.744727
28	1-{[5-(4-fluorobenzyl)- 3-pyridin-4-yl-1H- pyrazol-1-yl]acetyl}-N- methylpyrrolidin-3- amine		0.046	7.337242
29	[(2R)-1-{[5-(4- fluorobenzyl)-3-pyridin-4-yl-1H- pyrazol-1-yl]acetyl}pyrrolidin-2-yl]methanol		0.0175	7.756962
30	1-{[5-(4-fluorobenzyl)- 3-pyridin-4-yl-1H- pyrazol-1-yl]acetyl}azetidin-3-ol		0.0108	7.966576

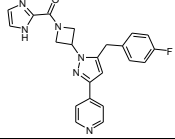|				
31	N-(1-(2-[5-(4- fluorobenzyl)-3- pyridin-4-yl-1H- pyrazol-1- yl]acetyl}piperidin-4- yl)propanamide		0.0105	7.978811
32	N-(1-(2-[5-(4- fluorobenzyl)-3- pyridin-4-yl-1H- pyrazol-1- yl]acetyl}piperidin-4- yl)ethanesulfonamide		0.012	7.920819
33	isopropyl (1-{[5-(4- fluorobenzyl)-3- pyridin-4-yl- 1H- pyrazol-1- yl]acetyl}piperidin-4- yl)methylcarbamate		0.006	8.221849
34	ethyl (1-{[5-(4- fluorobenzyl)-3- pyridin-4-yl-1H- pyrazol-1- yl]acetyl}piperidin-4- yl)methylcarbamate		0.009	8.045757
35	isopropyl (1-{[5-(4- fluorobenzyl)-3- pyridin-4-yl- 1H- pyrazol-1- yl]acetyl}piperidin-4- yl)carbamate		0.01	8
36	3-ethyl-1-(1-{[5-(4- fluorobenzyl)-3- pyridin-4-yl- 1H- pyrazol-1- yl]acetyl}piperidin-4- yl)-1- methylurea		0.004	8.39794
37	1-(1-{[5-(4- fluorobenzyl)-3- pyridin-4-yl-1H- pyrazol-1- yl]acetyl}piperidin-4- yl)-1,3- dimethylurea		0.011	7.958607

38	3-(1-{[5-(4- fluorobenzyl)-3- pyridin-4-yl-1H- pyrazol-1-yl]acetyl}piperidin-4- yl)-1,3-oxazolidin-2- one		0.00837	8.077275
39	4-[1-{2-[4-(1,1-dioxidoisothiazolidin- 2-yl)piperidin-1-yl]-2- oxoethyl}-5-(4- fluorobenzyl)-1H- pyrazol-3-yl]pyridine		0.017	7.769551
40	methyl (1-{[5-(4- fluorobenzyl)-3- pyridin-4-yl-1H- pyrazol-1-yl]acetyl}azetidin-3-yl)carbamate		0.025	7.60206
41	N-(1-{2-[5-(4- fluorobenzyl)-3-pyridin-4-yl-1H- pyrazol-1-yl]acetyl}azetidin-3- yl)methane sulfonamide		0.022	7.657577
42	N-(1-{2-[5-(4- fluorobenzyl)-3-pyridin-4-yl-1H- pyrazol-1-yl]acetyl}azetidin-3-yl)acetamide		0.041	7.387216
43	1-(1-{[5-(4- fluorobenzyl)-3-pyridin-4-yl-1H- pyrazol-1-yl]acetyl}pyrrolidin-3- yl)-1,3-dimethylurea		0.066	7.180456
44	methyl [(3S)-1-{[5-(4-fluorobenzyl)-3- pyridin-4-yl-1H- pyrazol-1-yl]acetyl}pyrrolidin-3-yl]carbamate		0.032	7.49485
45	1-{[5-(4-fluorobenzyl)- 3-pyridin-4-yl-1H- pyrazol-1-yl]acetyl}-4- [2-(methylsulfonyl)ethyl]piperazine		0.0139	7.856985

46	1-acetyl-4-{[5-(4-fluorobenzyl)-3- pyridin-4-yl-1H- pyrazol-1-yl]acetyl}piperazine		0.0169	7.772113
47	2-[5-(4-fluorobenzyl)- 3-pyridin-4-yl-1H- pyrazol-1-yl]-N-(cis-4- hydroxycyclohexyl)-N- methylacetamide		0.00867	8.061981
48	4-(1-{[5-(4- fluorobenzyl)-3-pyridin-4-yl-1H- pyrazol-1-yl]acetyl}piperidin-4-yl)morpholine		0.0101	7.995679
49	4-[5-(4-Fluoro-benzyl)-1-(1-methanesulfonyl-azetidin-3-yl)-1H-pyrazol-3-yl]-pyridine		0.375	6.425969
50*	1-{[5-(4-fluorobenzyl)-3-pyridin-4-yl-1H-pyrazol-1-yl]acetyl}-N-methylpiperidin-4-amine		0.073	7.136677
51*	4-{5-(4-fluorobenzyl)-1-[1-(1H-imidazol-2-ylcarbonyl)azetidin-3-yl]-1H-pyrazol-3-yl }pyridine		0.027	7.568636
52*	2-[5-(4-fluorobenzyl)- 3-pyridin-4-yl-1H- pyrazol-1-yl]-N-(2- morpholin-4-ylethyl)acetamide		0.044	7.356547
53*	N-(2-amino-2- methylpropyl)-2-[5-(4- fluorobenzyl)-3- pyridin-4-yl-1H- pyrazol-1-yl]acetamide		0.064	7.19382
54*	2-[5-(4-fluorobenzyl)- 3-pyridin-4-yl-1H- pyrazol-1-yl]-N-[(2S)- 2-hydroxypropyl]acetamide		0.028	7.552842

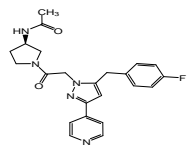|				
55*	2-({3-[5-(4- fluorobenzyl)-3- pyridin-4-yl-1H- pyrazol-1- yl]azetidin- 1- yl}carbonyl)pyrimidine		0.091	7.040959
56*	4-(5-{[5-(4- fluorobenzyl)-3- pyridin-4-yl-1H- pyrazol-1- yl]methyl}- 1,2,4-oxadiazol-3- yl)morpholine		0.019	7.721246
57*	N-[2-(acetylamino)-2- methylpropyl]-2-[5-(4- fluorobenzyl)-3- pyridin-4-yl- 1H- pyrazol-1- yl]acetamide		0.034	7.468521
58*	[(2S)-1-{[5-(4- fluorobenzyl)-3- pyridin-4-yl-1H- pyrazol-1- yl]acetyl}pyrrolidin-2- yl]methanol		0.0511	7.291579
59*	N-(1-{[5-(4- fluorobenzyl)-3- pyridin-4-yl-1H- pyrazol-1- yl]acetyl}pyrrolidin-3- yl)-N- methylacetamide		0.032	7.49485
60*	N-[(3R)-1-{2-[5-(4- fluorobenzyl)-3- pyridin-4-yl- 1H- pyrazol-1- yl]acetyl}pyrrolidin-3- yl]acetamide		0.044	7.356547
61*	4-(1-{[5-(4- fluorobenzyl)-3- pyridin-4-yl-1H- pyrazol-1- yl]acetyl}azetidin-3- yl)morpholine		0.045	7.346787
62*	1-(1-{[5-(4- fluorobenzyl)-3- pyridin-4-yl-1H- pyrazol-1- yl]acetyl}azetidin-3- yl)-3- methylurea		0.034	7.468521
63*	methyl (1-{[5-(4- fluorobenzyl)- 3- pyridin-4-yl-1H- pyrazol-1- yl]acetyl}pyrrolidin-3- yl)methylcarbamate		0.022	7.657577

64*	4-[5-(4-fluorobenzyl)- 1-{2-[3-(methylsulfonyl)- pyrrolidin-1-yl]- 2-oxoethyl}- 1H-pyrazol-3-yl]pyridine		0.023	7.638272
65*	1-{[5-(4-fluorobenzyl)-3-pyridin-4-yl-1H-pyrazol-1-yl]acetyl}-4-morpholin-4-ylazepane, maleic acid salt		0.023	7.638272

*indicates test set molecule

Alignment procedure

One of the fundamental assumptions wherein 3D-QSAR studies are based is that a geometric similarity should exist between the structures. In the present study the MOPAC geometry optimized structures were aligned on the template 36 which is the most active molecule among the given set. All the molecules were aligned by the Align Database command available in SYBYL using maximum substructure. It adjusts the geometry of the molecules such that its steric and electrostatic fields match the fields of the template molecule. The aligned molecules are shown in Figure 1.
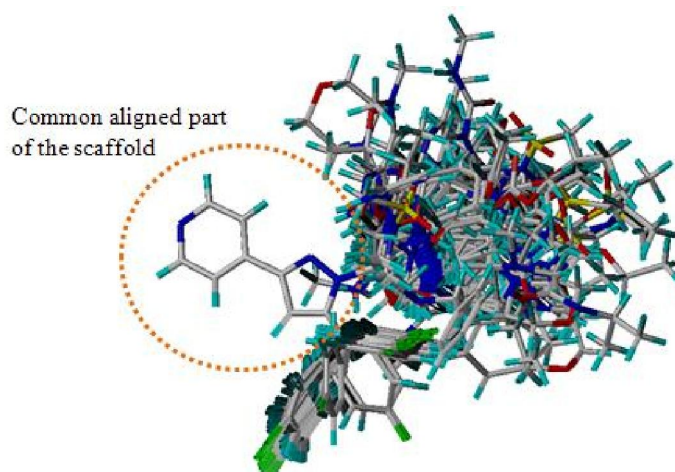
Figure 1
Alignment of all molecules: Blue indicates nitrogen, red indicates oxygen, yellow refers to sulfur, gray indicates carbon, and cyan indicates hydrogen.

CoMFA

The steric and electrostatic CoMFA potential fields were calculated at each lattice intersection of a regularly spaced grid of 2.0 A°. The grid box dimensions were determined automatically in such a way that region boundaries were extended beyond 4 A° in each direction from co-ordinates of each molecule. The van dar Waals potentials and Columbic terms, which represent steric and electrostatic fields, respectively, were calculated using tripos force field. A sp3 hybridized carbon atom with þ1 charge served as probe atom to calculate steric and electrostatic fields.

In the present study, CoMFA similarity indices descriptors were calculated. The similarity index $A_{F,k}$ for a molecule j with atoms *i* at *a* grid point *q* can be calculated as follows:

$$A_{F,k}^q(j) = -\sum_i \omega_{probe,k} \omega_{ik} e^{-ar_{iq}^2} \qquad (1)$$

Where ω_{ik} is the actual value of the physicochemical property *k*, which is evaluated using the probe atom $\omega_{Probe,k}$. At each grid point, a similarity index between the grid point *q* and each atom *i* of the molecule was calculated using Gaussian-type distance dependence. The default value of 0.3 was used as the attenuation factor α, which showed the steepness of the Gaussian-type function.

PLS ANALYSIS

A partial least-squares (PLS) methodology [16, 17, 18], which is an extension of multiple regression analysis, was used for the 3D-QSAR. For PLS analysis the independent variables were the CoMFA and CoMSIA descriptors and pIC50 values were used as dependent variables. Before the PLS analysis, the CoMFA and CoMSIA columns were calculated and filtered by using column filtering. To reduce noise in model generation a minimum default column-filtering value (s) of 2.00 kcal/mol (CoMFA) and 1.00 kcal/mol (CoMSIA) was used so that only those descriptor energies with values greater than the

above described will be considered for PLS analysis. The cross-validation with Leave-One-Out (LOO) [19, 20] option was carried out to obtain the optimum number of components (ONC), which was used in the final analysis. Final analysis (non-cross-validated) was performed to calculate conventional r^2 using the optimum number components obtained from the leave-one-out cross-validation analysis. The predictive ability of the 3D-QSAR models was determined using formula:

$$r^2_{pred} = \frac{(SD - PRESS)}{SD}$$

Where SD is the sum of squared deviations between the biological activities of each molecule and the mean activity of the training set molecules and PRESS is the sum of squared deviations between the predicted and actual activity values for every molecule in the test set.

RESULTS AND DISCUSSION

CoMFA statistical details

The predictive 3D-QSARmodels were generated for the training set of 49 CYP450 3A4 inhibitors using default parameters of COMFA, as determined by cross validation. Reliability of the QSAR models was statistically validated using several statistical parameters, such as r^2, q^2 and r^2_{pred}. The CoMFA models yielded a good cross-validated correlation coefficient with LOO of 0.844 and with leave-many-out (q2 with 10 groups) was 0.751, thus the predictions obtained with these models were reliable. These internal validation methods (leave-one-out and leave-one-out) determine the stability of the developed models.

The non-cross-validated PLS analysis gave a good correlation coefficient r^2 of 0.992 with a standard error of estimate (SEE) of 0.041. Cross validated r2 of 0.70, F-value stands for the degree of statistical confidence on the developed models and the model has good value of 1005.863. The steric and electrostatic contributions are 55.4% and 44.6%, respectively. Figure 2 shows the graph of actual versus predicted pIC50 values of the

compounds using CoMFA model. The statistical data obtained from the standard CoMFA model constructed with steric and electrostatic fields are depicted in **Table 2**. Experimental activities, predicted activities and residual values of the training set and test set by CoMFA model were given in Table 3 and 4.
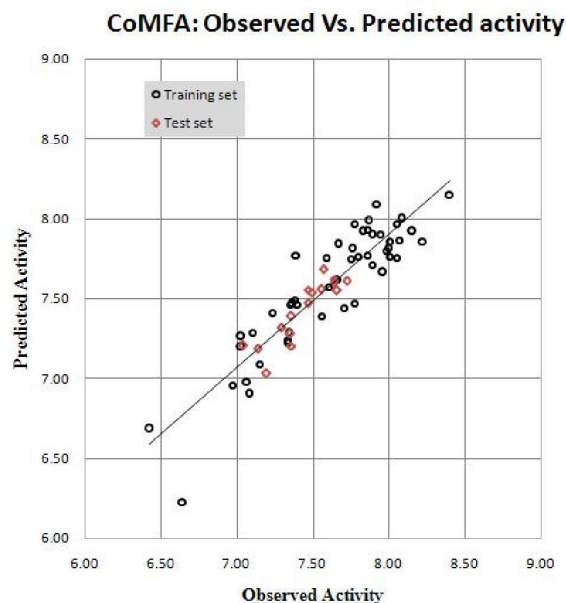
Figure 2

Plot of predicted versus observed pIC50 values derived from the steric/electrostatic CoMFA affinity model of the training (in blue) and test (in red) sets of PTS ligands.

TABLE 2: PLS STATISTICS OF COMFA AND COMSIA 3D-QSAR MODELS

	$q2$	$r2$	$r2pred$	$r2bs$	n	F value	SEE	Steric	Electrostatic
COMFA	0.844	0.992	0.783	0.992	5	1005.863	0.041	0.554	0.446

Validation of CoMFA model

Tropsha. et. al., have emphasized that having such a high value for goodness-of-fit and cross-validated correlation coefficient r2 (q2) >0.5 is insufficient for judging about the predictive power of a model. Although a high q2 value is vital, it cannot guarantee the

predictive power of a model [21, 22] Therefore, an external test set is necessary. An ideal QSAR model must also have accurate prediction on the external set. [21] The best model should also predict the activities well, for the compounds which are not included in the training set. A test set of 16 compounds, having wide range of activities was considered for external prediction (r^2_{pred}). The test compounds are in good agreement with the observed activity within a tolerable error range and substantiated by the r^2_{pred} value of 0.783 for CoMFA. Figure 2 shows that the CoMFA model is reliable and can be useful in designing new potent PTS inhibitors.

TABLE 3: RESIDUALS OF PREDICTIONS OF THE TRAINING SET BY THE COMFA MODEL.

S.No	PIC50	PREDICTED	RESIDUAL
1	7.026	7.266	-0.24
2	8	7.768	0.232
3	7.661	7.843	-0.182
4	7.886	7.715	0.171
5	7.886	7.902	-0.016
6	8.045	7.757	0.288
7	8.15	7.922	0.228
8	7.939	7.903	0.036
9	7.86	7.99	-0.13
10	6.642	6.228	0.414
11	7.075	6.907	0.168
12	7.346	7.465	-0.119
13	7.065	6.983	0.082
14	7.101	7.292	-0.191
15	7.331	7.235	0.096
16	7.331	7.221	0.11
17	7.148	7.093	0.055
18	7.552	7.395	0.157
19	7.366	7.47	-0.104

20	7.025	7.2	-0.175
21	7.698	7.445	0.253
22	7.795	7.764	0.031
23	7.397	7.467	-0.07
24	7.229	7.415	-0.186
25	7.376	7.493	-0.117
26	7.585	7.759	-0.174
27	7.744	7.75	-0.006
28	7.337	7.288	0.049
29	7.756	7.814	-0.058
30	6.966	6.962	0.004
31	7.978	7.803	0.175
32	7.92	8.096	-0.176
33	8.221	7.86	0.361
34	8.045	7.97	0.075
35	8	7.862	0.138
36	8.397	8.153	0.244
37	7.958	7.668	0.29
38	8.077	8.003	0.074
39	7.769	7.475	0.294
40	7.602	7.577	0.025
41	7.657	7.617	0.04
42	7.387	7.773	-0.386
43	7.823	7.923	-0.1
44	7.856	7.774	0.082
45	7.856	7.932	-0.076
46	7.772	7.971	-0.199
47	8.061	7.87	0.191
48	7.995	7.813	0.182
49	6.425	6.686	-0.261

TABLE 4: RESIDUALS OF PREDICTIONS OF THE TEST SET BY THE COMFA MODEL.

S.No	PIC50	PRED	RESIDUAL
50	7.638	7.6	0.038
51	7.136	7.188	-0.052
52	7.568	7.685	-0.117
53	7.356	7.389	-0.033
54	7.193	7.034	0.159
55	7.552	7.557	-0.005
56	7.04	7.208	-0.168
57	7.721	7.608	0.113
58	7.468	7.472	-0.004
59	7.291	7.316	-0.025
60	7.494	7.541	-0.047
61	7.356	7.203	0.153
62	7.346	7.28	0.066
63	7.468	7.556	-0.088
64	7.657	7.549	0.108
65	7.638	7.62	0.018

Interpretation of contour maps

CoMFA:

The steric and electrostatic contour maps for CYP450 3A4 enzyme system inhibitory model are displayed in the Figure 3 and 4. The steric map shows two large sized yellow contours around Acetaldehyde group connecting Piperidine and pyrazole rings, disfavoring bulky groups in these regions. In compounds 10, 11, 30, 49 and 55. Substitution of Azetidin at this position shows detrimental effect on inhibitory potency. Similarly compounds 13 and 20 with oxadiazole ring. Compound 14 also exhibits minimal activity due to the presence of urea group. Another small sized yellow contour around 1-ethyl 3-methyl urea group also disfavors substitution of methyl group in this

region. Compound 50, substituted with methyl amine at this position has less activity. In the contour map, one medium sized green contour runs around 1,3 dimethyl urea group, indicating that substitution of a methylformamide group on the piperidine ring has led to a great increase of inhibitor potency, compounds 6, 7, 33, 34 and 36 with methyl formamide group on the piperidine ring has great increase of inhibitor potency.

The electrostatic plot shows two small blue and one large blue contour around the Piperidine ring suggesting that substitution with positively charged group increases activity. This explains compound 6 reduced activity compared to 7. Big blue contour (Figure 4) around the piperidine ring, favors negative inductive effect (–I) groups viz. NO_2, NR and OR. This pattern can be observed in compounds 2, 6, 7, 33, 34, 35, 36, 38 and 47. Compounds having strong –I groups like NO_2, NR exhibit less activity than weak –I groups such as OR. Two small red contours are seen around acetaldehyde group indicating that substitution with more electronegative group increases activity. Compound 36 with oxygen exhibits high activity compared with compound 35 which has less electronegative nitrogen in the same place.
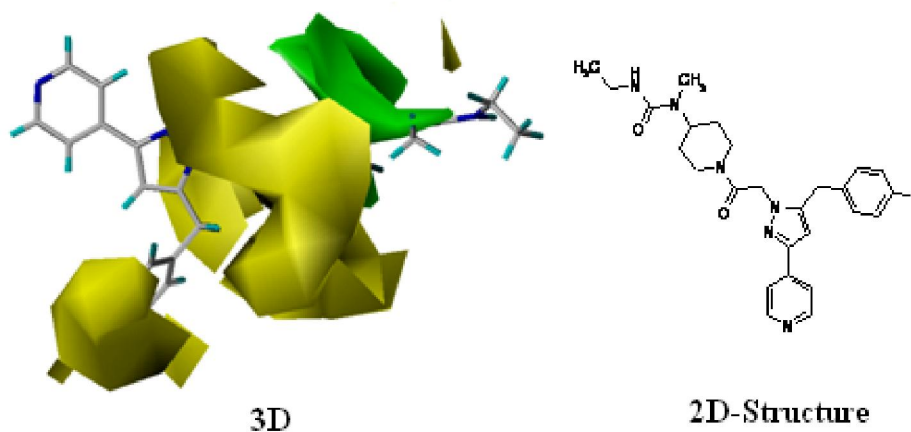

Figure 3
CoMFA Steric field contour map with best active compound 36.

The green contours indicate steric favored regions whereas the yellow contours denote steric unfavorable regions.
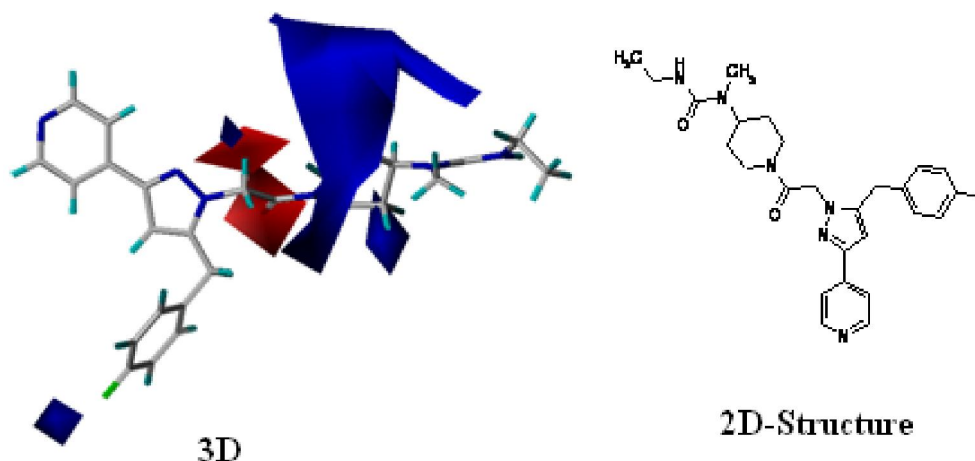
Figure 4
CoMFA electrostatic field contour map with best active compound 36.
The blue contours identify regions that favor electropositive substituent and the red regions favor electronegative substituent.

CONCLUSION

In this study, by using the alignment scheme generated from distill, highly predictive CoMFA was developed and used to predict the pIC50 activity of a set of CYP450 3A4 inhibitors. The QSAR models gave good statistical results in terms of q^2 and r^2 values, and have been validated using a test set, obtained from the hierarchical clustering. The CoMFA region focusing model provided the most significant correlation of steric and electrostatic fields with the biological activities. The analysis of CoMFA contour maps suggested that substitution of azetidin and oxadiazole rings at position of acetaldehyde will cause reduction in the activity. CoMFA contour maps favor the presence of

methylformamide group on Piperidine ring. This contributes to a great increase inhibitory activity. This comparative analysis of contour maps is expected to be of an aid in the design of compounds with an enhanced inhibitory activity and better selectivity to CYP450 3A4 enzyme system

REFERENCES

1. Planken Simon Paul, Sutton Scott Channing, Chen Rongliang: Therapeutic compounds, Patent number; US7919488B2

2. J. Burton, I. Ijjaali, O. Barberan, F. Petitet, D.P. Vercauteren, A. Michel: Recursive partitioning for the prediction of cytochromes P450 2D6 and 1A2 inhibition: importance of the quality of the dataset. J. Med. Chem. 2006; 49: 6231–6240

3. N. Manga, J.C. Duffy, P.H. Rowe, M.T. Cronin: Structure-based methods for the prediction of the dominant P450 enzyme in human drug biotransformation: consideration of CYP3A4, CYP2C9, CYP2D6. SAR QSAR Environ. Res. 2005; 16: 43–61.

4. S. Ekins, J. Berbaum, R.K. Harrison: Generation and validation of rapid computational filters for cyp2d6 and cyp3a4. Drug Metab. Dispos. 2003; 31: 1077–1080.

5. L.C. Wienkers, T.G.: Predicting in vivo drug interactions from in vitro drug discovery data.. Heath, Nat. Rev. Drug Discovery 2005; 4: 825–833.

6. H. Park, S. Lee, J. Suh: Structural and dynamical basis of broad substrate specificity, catalytic mechanism, and inhibition of cytochrome P450 3A4. J. Am. Chem. Soc. 2005; 127: 13634-13642.

7. Blum, D. J. W., and R. E. Speece: Determining chemical toxicity to aquatic species. Environ. Sci. Technol. 1990; 24: 284-293.

8. R.D. Cramer III, D.E. Patterson, J.D. Bunce: Comparative molecular field analysis (CoMFA). 1. Effect of shape on binding of steroids to carrier proteins. J. Am. Chem. Soc. 1998; 110 : 5959-5967.

9. G.R. Desiraju, B. Gopalakrishnan, R.K. Jetti, A. Nagaraju, J.D. Raveendra, A. Sharma, M.E. Sobhia, R. Thilagavathi: Computer-aided design of selective COX-2 inhibitors: comparative molecular field analysis, comparative molecular similarity indices analysis, and docking studies of some 1,2-diarylimidazole derivatives. J. Med. Chem. 2002; 45: 4847-4857.

10. S.K. Singh, N. Dessalew, P.V. Bharatam: 3D-QSAR CoMFA study on indenopyrazole derivatives as cyclin dependent kinase 4 (CDK4) and cyclin dependent kinase 2 (CDK2) inhibitors. Eur. J. Med. Chem. 2006; 41: 1310-1319

11. Sybyl 6.7.1, Tripos Inc., 1699 South Hanely Road, St. Louis, Missouri, 63144, USA.

12. Clark M and Cramer R D: Validation of the general purpose Tripos 5.2 forcefield. J. Comput. Chem. 1989; 10: 982-1012.

13. Gasteiger, J, Marsili, M.: Iterative partial equalization of orbital electronegativity – a rapid access to atomic charges. Tetrahedron. 1980; 36: 3219-3228.

14. J. J. J. Stewart: MOPAC: A semi empirical molecular orbital program. Comput. Aided Mol. Des. 1990; 4: 1-105.

15. Oprea, T. I.; Waller, C. L.; Marshall, G. R: Three-dimensional quantitative structure-activity relationship of human immunodeficiency virus (I) protease inhibitors. 2. Predictive power using limited exploration of alternate binding modes. J. Med. Chem. 1994; 37: 2206-2215.

16. Wold S, Ruhe A, Wold H, Dunn WI: The collinearity problem in linear regression. The partial least squares approach to generalized inverses. SIAM J. Sci. Stat. Comput. 1984; 5: 735-743.

17. Clark M., Cramer R.D., III: The probability of chance correlation using partial least squares (PLS). Quant. Struct. Act. Relat. 1993;12:137-145.

18. Bush B.L., Nachbar R.B., Jr: Sample-distance partial least squares: PLS optimized for many variables, with application to CoMFA. J. Comput. Aided Mol. Des. 1993;7: 587-619.

19. R.D. Cramer III, J.D. Bunce, D.E. Patterson: Crossvalidation, bootstrapping, and partial least squares compared with multiple regression in conventional QSAR studies. Quant. Struct. Act. Relat.1988; 7: 18-25.

20. S Wold: Cross-validatory estimation of the number of components in factor and principal components analysis. Technometrics, 1978; 20: 397-405.

21. Golbraikh A, Tropsha A.: Beware of q2!. J Mol Graph Model. 2002; 20: 269-276.

22. Tropsha A, Gramatica P, Gombar VK.: The importance of being Earnest: Validation is the absolute essential for successful application and interpretation of QSPR models. QSAR Comb Sci. 2003; 22: 69-77.

For Correspondence:
Ravi Shekar Ananthula
Email: ravini8797@gmail.com